A revised SALT2 surface for fitting Type Ia supernova light curves

G. Taylor [1]★ C. Lidman [1], B. E. Tucker,[1,2,3] D. Brout,[4]† S. R. Hinton [5] and R. Kessler[6,7]

[1]*Research School of Astronomy and Astrophysics, Australian National University, Canberra 2611, Australia*

[2]*National Centre for the Public Awareness of Science, the Australian National University, Canberra 2601, Australia*

[3]*The ARC Centre of Excellence for All-Sky Astrophysics in 3 Dimensions (ASTRO 3D), Australia*

[4]*Department of Physics and Astronomy, University of Pennsylvania, Philadelphia, PA 19104, USA*

[5]*School of Mathematics and Physics, University of Queensland, Brisbane, Australia*

[6]*Department of Astronomy and Astrophysics, University of Chicago, Chicago, IL 60637, USA*

[7]*Kavli Institute for Cosmological Physics, University of Chicago, Chicago, IL 60637, USA*

ABSTRACT

We present a revised Spectral Adaptive Light Curve Template (SALT2) surface (SALT2-2021) for fitting the light curves of Type Ia supernovae (SNe Ia), which incorporates new measurements of zero-point calibration offsets and Milky Way extinction. The most notable change in the new surface occurs in the UV region. This new surface alters the distance measurements of SNe Ia, which can be used to investigate the nature of dark energy by probing the expansion history of the Universe. Using the revised SALT2 surface on public data from the first 3 yr of the Dark Energy Survey Supernova Program (combined with an external low-z SNe Ia sample) and combining with cosmic microwave background constraints, we find a change in the dark energy equation-of-state parameter, $\Delta w = 0.015 \pm 0.004$. This result highlights the continued importance of controlling and reducing systematic uncertainties, particularly with the next generation of supernova analyses aiming to improve constraints on dark energy properties.

Key words: supernovae: general – dark energy.

1 INTRODUCTION

Type Ia supernovae (SNe Ia) are important cosmological probes that are used as distance estimators to help constrain the nature of dark energy (see e.g. Howell 2011 for a review). SNe Ia are standardisable candles, displaying an empirical relationship between their peak luminosity, and their light-curve width (or 'stretch') and colour (Pskovskii 1977; Phillips 1993; Riess, Press & Kirshner 1996; Tripp 1998). This two-parameter luminosity correction is the most common technique for standardising a set of SNe Ia. By fitting a light-curve model to time-series photometry of SNe Ia we recover the SN parameters (amplitude, stretch, and colour), and infer their distances. The accuracy at which light curves can be modelled directly impacts these distances, and moreover, cosmological constraints.

Spectral Adaptive Light Curve Template (SALT2; Guy et al. 2007) is an empirical spectro-photometric model that is used in most modern SN Ia analyses, including the SuperNova Legacy Survey 3 yr analysis (SNLS; Conley et al. 2011), the Joint Light Curve Analysis (JLA; Betoule et al. 2014), the Pantheon analysis (Scolnic et al. 2018), the Pan-STARRS1 analysis (PS1; Jones et al. 2018), and the Dark Energy Survey 3 yr analysis (DES–SN3YR; Abbott et al. 2019). The SALT2 model consists of two phase-dependent components and a phase-independent colour law, an instance of which called the SALT2 surface. The SALT2 surface is determined through a training process. The most recent surface is SALT2.4 (hereafter referred to as SALT2-2014), which was produced for JLA, and is publicly available.[1] Since 2014 there has been a consensus in the literature for using a revised Galactic dust extinction map, and there have also been improvements in photometric calibrations of some SNe Ia. Dust extinction and calibration are both key inputs to the SALT2 model that will affect the resulting SALT2 surface.

The amount of extinction caused by dust in our Milky Way has been revised by Schlafly et al. (2010) and Schlafly & Finkbeiner (2011). They find an overprediction of reddening in the Schlegel, Finkbeiner & Davis (1998) dust maps, and therefore recommend a 14 per cent re-calibration of Milky Way extinction as a correction. Changes in the amount of reddening caused by Milky Way dust affect the colour of SNe Ia, which is an important parameter when fitting SN Ia distances. This re-calibration was not applied to the SNe Ia used to train SALT2-2014.

Using the PanSTARRS1 calibration covering 3/4 of the sky, the flux zero-points of some of the SNe Ia used in the training of SALT2-2014 have been updated by an average of 10 mmag (Scolnic et al. 2015). The systematic uncertainty in cosmological parameters arising from our imperfect knowledge of photometric systems and their zero-points is significant. In the JLA, Pantheon, and DES–SN3YR samples, this uncertainty contributes between a quarter and two-thirds of the total systematic uncertainty (Betoule et al. 2014; Scolnic et al. 2018; Brout et al. 2019b; Jones et al. 2019).

★ E-mail: gtaylor@mso.anu.edu.au

† NASA Einstein Fellow.

[1]http://supernovae.in2p3.fr/salt/doku.php

These improvements in Galactic extinction and photometric calibration are particularly important because statistical and systematic uncertainties are comparable in SN Ia cosmology analyses (Suzuki et al. 2012; Scolnic et al. 2014), and the current SALT2 surface has been identified as a limiting factor. For example, the SALT2 model uncertainty contributes $\sigma_w^{sys} = 0.009$ in Brout et al. (2019b), 0.008 in Jones et al. (2018), and 0.023 in Jones et al. (2019). Current SN Ia cosmology analyses and future surveys therefore require an improved SALT2 surface to make the most of their high-quality data and improve measurements of dark energy properties. Future surveys that focus on producing a large SN sample from a single instrument can also benefit from an updated SALT2 surface, as they will see the effects of the new surface.

Here, we update the SALT2 surface using recent improvements in calibration and Galactic extinction to produce a new surface, SALT2-2021.[2] When using SALT2-2021, the revised Galactic extinction map and Supercal calibration adjustments should be applied to the data used for light curve fitting. We include an overview of the SALT2 model, including the training and fitting processes (Section 2). We then describe the specific changes made to produce the SALT2-2021 surface (Section 3). We evaluate the impact of SALT2-2021 on cosmological distance measurements using the DES–SN3YR sample and simulations (Section 4), and discuss these results (Section 5).

2 SALT2

2.1 Model description

SALT2 is an empirical SNe Ia model (Guy et al. 2005, 2007). The model describes the spectro-photometric time evolution of a SN Ia, and was built using both spectroscopic and photometric data from a large set of nearby ($z \lesssim 0.1$) and distant ($0.2 \lesssim z \lesssim 0.8$) SNe Ia.

In SALT2, the spectral flux density for each SN Ia at a particular phase (p) and wavelength (λ) is given as

$$f_\lambda = x_0 \times [M_0(p,\lambda) + x_1 M_1(p,\lambda) + \ldots]$$
$$\times \exp[cCL(\lambda)], \tag{1}$$

where amplitude (x_0), stretch (x_1), and colour (c) are parameters determined from a light curve fit for each SN Ia; M_0 and M_1 are phase-dependent components of the SALT2 model; and CL is the phase-independent SALT2 colour law. Specifically, M_0 describes the mean spectral energy distribution (SED) of a SN Ia, while M_1 describes the first-order deviation around this SED.

The SALT2 model does not fully describe all the observed SN Ia variability – the remaining variability (~ 0.1 magnitudes) is often labelled as 'intrinsic scatter'. Scatter in the SN population itself can have coherent and chromatic contributions. To simulate distance biases, commonly used intrinsic scatter models are from Kessler et al. (2013) – these models are based on Guy et al. (2010; ~ 75 per cent coherent contributions, ~ 25 per cent chromatic contributions), and Chotard et al. (2011; ~ 25 per cent coherent contributions, ~ 75 per cent chromatic contributions). Currently, there is no strong evidence favouring one model over the other.

To understand the origins of the scatter and to further improve SNe Ia as standard candles, a number of studies have looked for and found evidence for relationships between the properties of the SN and its host galaxy. Relationships have been found between the luminosity of a SN Ia and its host galaxy metallicity, morphological type, and

mass (Hamuy et al. 2000; Wang et al. 2006; Kelly et al. 2010; Sullivan et al. 2010; Smith et al. 2020). Scolnic et al. (2020) use a different approach and consider the properties of SN Ia 'siblings' (i.e. SNe Ia that share the same parent galaxies) and find at least 50 per cent of the intrinsic scatter of SNe Ia distance modulus residuals does not originate from common host properties, albeit using a sample of only eight pairs of SN Ia siblings. A similar study of two SNe Ia in the same galaxy (NGC 3972) finds significant luminosity differences between SNe Ia with similar light-curve shapes and colours, reaffirming that the popular two-component parametrization (as in SALT2) does not fully describe SNe Ia (Foley et al. 2020) without intrinsic scatter.

An additional complication from host galaxies is their dust extinction (reddening) contribution. As it is difficult to disentangle the effects of dust and the intrinsic relation between SN colour and brightness (Nobili et al. 2003), contributions from both are implicitly included in the colour (c) parameter and colour law (CL) of SALT2.

Alternatives to SALT2 have different approaches to light curve modelling. We briefly outline some differences between SALT2 and other common models. More in-depth comparisons between light curve models can be found in the literature (e.g. Kessler et al. 2009b; Bengochea 2013). We focus on SALT2 as it is publicly available and is widely used in SN analyses (e.g. JLA, Pantheon, DES).

MLCS2K2 (Jha, Riess & Kirshner 2007) and SNooPy (Burns et al. 2011) attempt to explicitly separate reddening by dust from phase-dependent intrinsic colour, whereas SALT2 combines both effects into one colour parameter. SiFTO (Conley et al. 2008) performs similar to SALT2, but differs with respect to SALT2 in the way colour and stretch are treated (see Guy et al. 2010 for details). SUGAR (Léget et al. 2019) has more parameters than SALT2, and derives a colour law that is consistent with Milky Way extinction (whereas the SALT2 colour law differs significantly from the reddening from dust in the Milky Way).
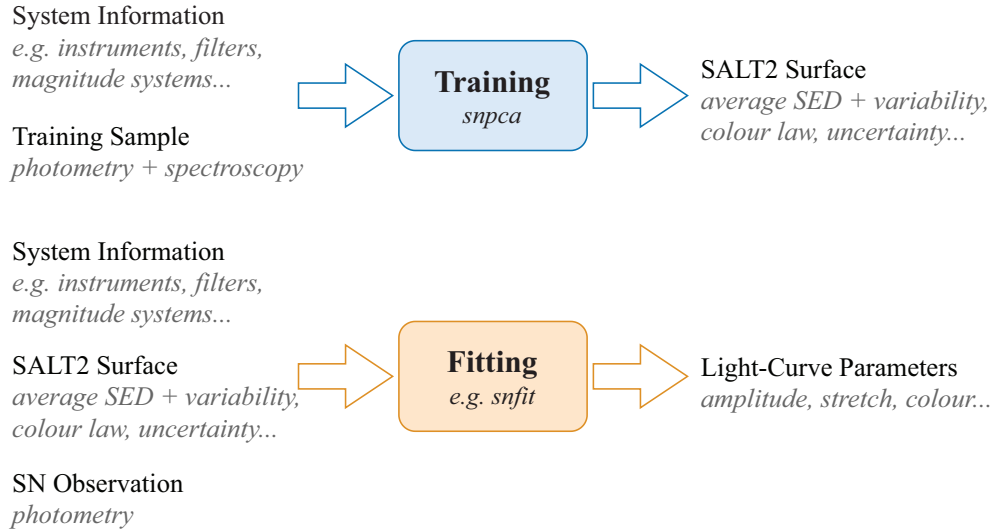
2.2 Training

The progenitor and explosion mechanisms leading to SNe Ia are areas of active research (Maoz, Mannucci & Nelemans 2014), and theoretical models producing SN Ia spectra are not yet good enough to be used for correcting SN Ia brightness. For these reasons, models are empirically determined from a training sample of real SN observations. The original SALT model (Guy et al. 2005) was developed into the current SALT2 model (Guy et al. 2007). Two widely used SALT2 surfaces have been released: SALT2.2, an SNLS release (Guy et al. 2010); and SALT2.4, released as part of the JLA of SNLS and SDSS-II SNe Ia (Betoule et al. 2014, here referred to as SALT2-2014).

SALT2 is trained on a sample of photometric and spectroscopic observations of both nearby and distant SNe Ia. Including spectral data improves modelling of spectral features that are hard to access using photometry alone, while including higher redshift SNe reduces the dependence on the nearby SNe sample and provides better constraints on the rest-frame ultraviolet regions of the spectrum (Bengochea 2013). This training sample, along with information on the instruments and magnitude systems, is passed to the snpca[3] training program, as shown in Fig. 1. The output of snpca is a SALT2 surface, i.e. an iteration of the SALT2 model. For a detailed description of the training process, see Mosher et al. (2014).

---

[2]Available from 10.5281/zenodo.4646495.

[3]We use v2.3.22, which was kindly provided to us by Marc Betoule.

Figure 1. An illustration of the inputs and outputs of the SALT2 training and fitting processes. The training of the global SALT2 model produces a SALT2 'surface', which is used as an input for light curve fitting. The recovered light-curve parameters are therefore dependent on the SALT2 surface used. The surface needs to be recomputed when the inputs, e.g. magnitude systems, are revised.

2.3 Fitting light curves, distances, and cosmology

A SALT2 surface is passed to a light curve fitting program to fit light curves to photometric time-series observations of SNe. Available fitting programs include `snfit`,[4] `SNANA`,[5] and `SNCosmo`.[6] This fit produces the most likely light curve parameters x_0, x_1, and c from equation (1), together with their covariances. From here, distance moduli (μ) are obtained using the Tripp equation (Tripp 1998):

$$\mu = m_B - M + \alpha x_1 - \beta c, \qquad (2)$$

where $m_B = -2.5\log(x_0)$, M represents the absolute magnitude of a SN Ia with $c = x_1 = 0$, and α and β are nuisance parameters representing the slopes of the stretch-luminosity and colour–luminosity relations. The nuisance parameters (α, β, M) can be determined together with cosmological parameters (e.g. Guy et al. 2005; Betoule et al. 2014), or in a separate step before the cosmological parameters are fitted (e.g. `SALT2mu`, Marriner et al. 2011; `BBC`, Kessler & Scolnic 2017).

Some modifications to the Tripp equation (in the form of an additional 'mass-step' term) have been used to account for the observed correlation between SN brightness and host-galaxy properties, e.g. Kelly et al. (2010), Sullivan et al. (2010). Following Brout et al. (2019b), we include a mass-step correction ($\delta\mu_{\text{host}}$). We also include a 5D bias-correction term from `BBC` ($\delta\mu_{\text{bias}}$), which uses detailed simulations to predict biases from selection effects. The modified version of the Tripp equation used in this work is therefore

$$\mu = m_B - M + \alpha x_1 - \beta c - \delta\mu_{\text{host}} - \delta\mu_{\text{bias}}. \qquad (3)$$

3 IMPROVEMENTS IN THE NEW SURFACE (SALT2-2021)

We have produced a new surface denoted SALT2-2021 that implements two important updates to the model inputs. The underlying SALT2 model and code used to produce this surface are identical to

that used for SALT2-2014, with the exception that we sample the resulting surface more finely in wavelength.

3.1 Training sample

To compare our results with the previous SALT2-2014 surface (Betoule et al. 2014), we use the same training sample of SNe. This sample contains photometry and spectroscopy from 420 SNe Ia from various surveys, listed in Table 1. All 420 SNe Ia in the training sample have photometric data, but only 83 of those have spectral data. The phase and wavelength coverage of this spectral data is shown in Fig. 2. For more details on this training sample, see Betoule et al. (2014).

Altering the set of SNe used in the training sample is beyond the scope of this work, which focuses primarily on the effects of modifying the Milky Way dust extinction and photometric zero-points on the SALT2 surface. In future work, we will explore how the SALT2 surface changes when we add more recent SN Ia data.

3.2 Re-Scaled Milky Way extinction

A reddening *law* predicts the amount of absorption versus wavelength, relative to the absorption at a reference wavelength (typically the effective wavelength of the Bessell B band). A *dust map* predicts the reddening for the reference wavelength at any sky location. Together, a dust map and reddening law predict the amount of absorption at any wavelength, and any sky location.

When fitting a light curve, SALT2 uses the Cardelli, Clayton & Mathis (1989) reddening law to correct SNe Ia photometry for Milky Way extinction, with the colour excess $E(B - V)$ calculated from the Schlegel et al. (1998) dust maps.[7] A 14 per cent re-calibration of the Schlegel et al. (1998) dust map is prescribed in Schlafly et al. (2010) and Schlafly & Finkbeiner (2011). Until now, this re-calibration had not been applied to the SNe used to train SALT2. We implement this

---

[4]http://supernovae.in2p3.fr/salt/doku.php
[5]http://snana.uchicago.edu/
[6]https://sncosmo.readthedocs.io/

[7]The SALT2 colour law derived during the training process includes contributions from the intrinsic colour of an SN, as well as any host galaxy extinction.

Table 1. SNe Ia used in SALT2 training sample. Two SNe were observed by SDSS, CSP, and CfA3, and four SNe were observed by both SDSS and CfA3 – giving a total of 420 unique SNe Ia in the training sample.

Survey	Number of SNe	Redshift range
SDSS-II (Sako et al. 2018)	203	$0.1 \lesssim z \lesssim 0.3$
SNLS (Conley et al. 2011; Sullivan et al. 2011)	113	$0.2 \lesssim z \lesssim 0.9$
Calan/Tololo (Hamuy et al. 1996)	5	$z \lesssim 0.1$
CSP (Contreras et al. 2010)	2	$z \lesssim 0.1$
CfA1 (Riess et al. 1999)	8	$z \lesssim 0.1$
CfA2 (Jha et al. 2006)	14	$z \lesssim 0.1$
CfA3 (Hicken et al. 2009)	58	$z \lesssim 0.1$
Historical low z (Betoule et al. 2014 and references within)	25	$z \lesssim 0.1$
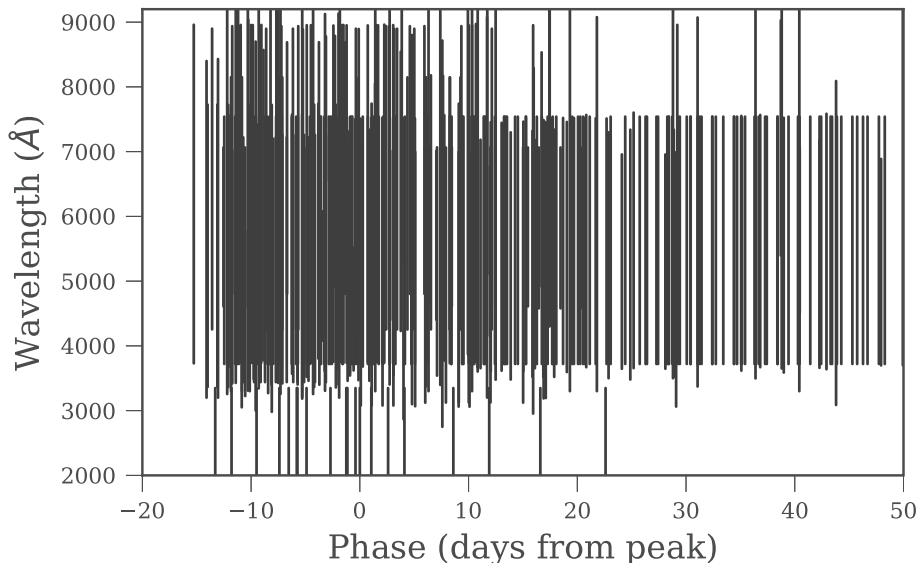
Figure 2. Wavelength coverage of the spectra used in the training sample, plotted as a function of phase.

re-calibration by adjusting the $E(B - V)$ of all the SNe in the SALT2 training sample by a factor of 0.86, such that

$$E(B - V)_{new} = 0.86 \times E(B - V)_{old}. \qquad (4)$$

The Schlafly & Finkbeiner (2011) dust maps are the most commonly used dust maps for supernova analyses (e.g. Burns et al. 2014; Scolnic et al. 2015; Foley et al. 2016; Holoien et al. 2016; Dimitriadis et al. 2018; Pierel et al. 2018; Scolnic et al. 2018; Kessler et al. 2019; Khetan et al. 2020; Mandel et al. 2020). Other dusts maps, for example, the dust map derived using data from the Planck satellite (Planck Collaboration XI 2014), differ slightly from the the map used here. We evaluate the impact of the dust maps by training a version of SALT2-2021 with Planck Collaboration XI (2014) dust maps (instead of Schlafly & Finkbeiner 2011) and re-running the analysis in Section 4. We find $\Delta w = 0.01$ compared to the results using the Schlafly & Finkbeiner (2011) map. This is a slightly smaller than the shift in w from adopting the revised zero-points and the re-calibration of the Schlafly & Finkbeiner (2011) dust maps.

3.3 Re-calibrated photometry

The SALT2-2014 surface is trained on SNe from a number of surveys (Section 3.1) with little or no overlapping sky area, and thus the calibration relies on a standard star system. The approach used by these surveys to calibrate the flux scale is not homogeneous.

This introduces systematic errors that can be difficult to quantify, and which propagate through to redshift-dependent distance biases (resulting in a w bias).

'Supercal' (Scolnic et al. 2015) improves the relative calibration by using tertiary standard stars in regions of survey overlap to determine the zero-point offset between each system and the PS1 system, which has a relative calibration uncertainty of <5 mmag (Schlafly et al. 2012; Chambers et al. 2016) – thus effectively re-calibrating each system. The effect of this re-calibration was to shift w by 0.026 for a combined sample that includes PS1, SNLS, and SDSS (Scolnic et al. 2015).

Until now, this re-calibration has only been applied to samples *fitted* with the SALT2 model; however, the SALT2-2014 surface has been *trained* without Supercal. We adjust the SALT2 training data to include the supercalibrated zero-points and retrain SALT2, to ensure consistent photometric calibration for future SN analyses. This re-calibration affected 390 of 420 SNe Ia in the training sample – the unaffected 30 SNe are from surveys that were not re-calibrated by Supercal. The adopted zero-point offsets are in table 5 of Scolnic et al. (2018).

3.4 Calibration uncertainties

In addition to the SALT2-2021 surface, we provide a suite of perturbed surfaces, where each perturbed surface has been trained with
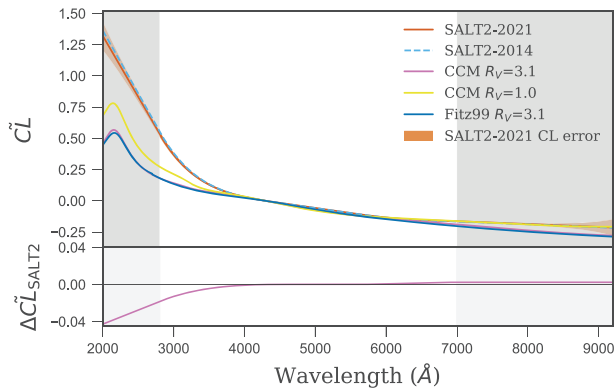
Figure 3. The derived colour law (*CL*) for the old *(cyan, dashed)* and new *(orange, solid)* SALT2 surfaces, for a $c = 0.1$ SN Ia, where $\tilde{CL} \equiv -cCL(\lambda)$ (for the SALT2 colour laws). The white region is the wavelength range over which the SALT2 colour law is fit, and the grey-shaded regions represent the wavelength ranges in which the SALT2 colour law is linearly extrapolated from the end points. Also plotted are common extinction laws from Cardelli et al. 1989 (CCM) and Fitzpatrick 1999 (Fitz99), for $E(B - V) = 0.1$, where $\tilde{CL} \equiv A(\lambda) - A(B)$ for the extinction laws. Differences between the SALT2-2021 and SALT2-2014 surfaces are shown in the lower panel.

a shift applied to one zero-point (0.01 mag) or 1 filter transmission curve (1 nm). These perturbed surfaces span all instruments and filter bands used in the training, and can be used to account for correlated systematic uncertainties in the training and light-curve fitting (e.g. see section 5.4 in B14). The perturbed surfaces are available online.[8]

3.5 Comparing SALT2-2021 and SALT2-2014

The SALT2-2021 colour law for a $c = 0.1$ SN Ia, plotted in Fig. 3, agrees with the SALT2-2014 colour law for wavelengths above $\sim$4000 Å. Below $\sim$4000 Å, there is some deviation. The SALT2 colour law differs significantly from the Cardelli et al. (1989) and Fitzpatrick (1999) colour laws (also plotted in Fig. 3), again, mainly in the region below $\sim$4000 Å. This difference is long-known and shows that there is an intrinsic component that has more impact in the UV than dust.

The average spectral energy distribution of the revised SALT2-2021 surface, plotted in Fig. 4, is in good agreement with the SALT2-2014 surface between $\sim$3000 and 8000 Å. There is a difference of a few per cent above $\sim$8000 Å, and much larger difference below $\sim$3000 Å, reaching 20 per cent in the UV part of the spectral energy distribution. This region ($\sim$2000 Å) is poorly sampled in the training set for SALT2 (as shown in Fig. 2) and therefore poorly constrained. These effects also correspond to the linearly-extrapolated region of the SALT2 colour law (the shaded region of Fig. 3), where the changes are greatest.

Fig. 5 shows the differences between the published SALT2-2014 surface, and various iterations of the new surface (trained with only Milky Way extinction modified, with only the zero-points modified, and with both modified). We are able to reproduce the original SALT2-2014 surface to within 0.1 per cent, giving us confidence in our training procedures (see Appendix A for details). The differences in the final SALT2-2021 spectral energy distribution are the sum of differences due to modifying the Milky Way extinction and modifying the photometric zero-points.
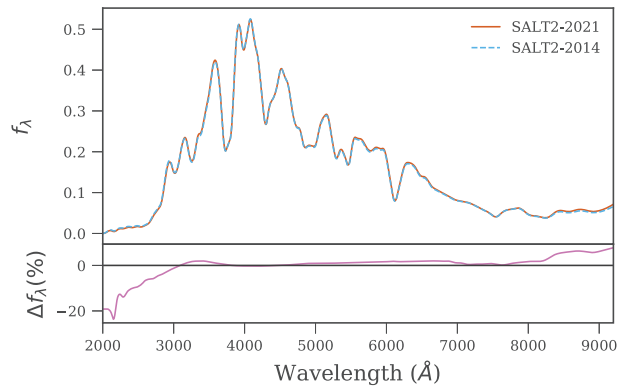
Figure 4. The trained spectral energy distribution of SNe Ia ($c = 0$, $x_1 = 0$) for the old *(cyan, dashed)* and new *(orange, solid)* SALT2 surfaces. The lower panel shows the difference in the average spectral energy distribution between the old and new SALT2 surfaces at each wavelength, where $\Delta f_\lambda (\text{per cent}) = 100 \times \frac{f_{\lambda 2021} - f_{\lambda 2014}}{f_{\lambda 2021}}$.
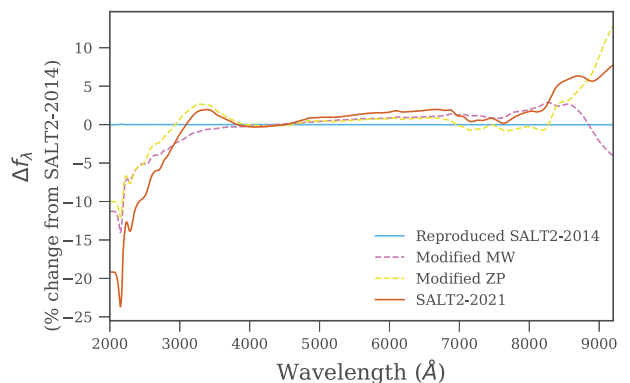
Figure 5. The difference in the spectral energy distribution between the SALT2-2014 surface, and: a reproduced version of SALT2-2014 for process verification *(cyan, Appendix A)*; a retrained surface with only re-scaled Milky Way extinction applied *(magenta, Section 3.2)*; a retrained surface with only re-calibrated zero-points applied *(yellow, Section 3.3)*; and the final SALT2-2021 surface with Milky Way and zero-point adjustments applied *(orange)*. We are able to reproduce the original SALT2-2014 surface to within 0.1 per cent, whereas the new SALT2-2021 surface has fractional changes of up to 20 per cent relative to SALT2-2014 (albeit at the low-flux ends of the spectrum).

4 FIRST ANALYSIS WITH SALT2-2021

4.1 The DES–SN3YR sample

The Dark Energy Survey (DES; The Dark Energy Survey Collaboration 2005) is a multiprobe investigation into the nature of dark energy, using DECam (Flaugher et al. 2015; Morganson et al. 2018) on the 4 m Blanco telescope at the Cerro Tololo Inter-American Observatory (CTIO). DES operated from 2013 to 2019 and collected data for a 5000 deg^2 wide-field survey, as well as a 27 deg^2 dedicated Dark Energy Survey Supernova Program (DES–SN; Bernstein et al. 2012). Over 30 000 transients were discovered with DES–SN, and light curves were measured in *griz* bands over a roughly weekly cadence (Kessler et al. 2015). A subset of these transients have been identified as SNe Ia, via either photometric ($\sim$3000 SNe from $0.01 \leq z \leq 1.2$) or spectroscopic ($\sim$500 SNe from $0.017 \leq z \leq 0.9$) classification (D'Andrea et al. 2018).

Table 2. Parameters of the DES–SN3YR SNe that did not pass our cuts. Values are from the published DES–SN3YR data.

SN	Sample	x_1	c	m_B	z	Cut at stage	Cut for surface
1298893	DES	-2.23698	-0.0279837	20.8162	0.1962	Light-curve fitting[a]	SALT2-2021
1330031	DES	0.022023	-0.128202	18.7782	0.104	Bias corrections[b]	SALT2-2014, SALT2-2021
1308884	DES	-1.42624	0.072173	19.0801	0.0772	Bias corrections	SALT2-2014, SALT2-2021
2002G	Low-z	-1.52225	0.2214	17.3307	0.03509	Bias corrections	SALT2-2014, SALT2-2021

Notes. [a]One object failed the light-curve fitting requirement $-20 \leq \text{TRESTMIN} \leq 0$.
[b]Three objects with no 5D bias corrections were rejected at the BBC stage. BBC was unable to determine bias correction because of limited MC coverage in this region of z, c, x_1.

The sample we analyse in this work is from the published set of 207 spectroscopically confirmed SNe Ia from the first 3 yr of the Dark Energy Survey, combined with a selection of 122 low-redshift SNe Ia (DES–SN3YR, Brout et al. 2019b), released as part of the Dark Energy Survey's Data Release I (Abbott et al. 2018)..[9] The external low redshift subset includes SNe Ia ($0.01 < z < 0.1$) from the Harvard-Smithsonian Center for Astrophysics surveys (CfA3, CfA4; Hicken et al. 2009, Hicken et al. 2012) and the Carnegie Supernova Project (CSP; Contreras et al. 2010, Stritzinger et al. 2011).

Though we begin with the full sample of 329 SNe from the DES–SN3YR sample, our results are subject to selection requirements (cuts) applied in different stages of the analysis. After these cuts are applied, we are left with 326 SNe using SALT2-2014, and 325 SNe using SALT2-2021 (the discarded SNe are given in Table 2). The difference in the number of SNe that pass cuts for each surface is due to SN1298893. Fitting SN1298893 with SALT2-2021 changed the recovered PEAKMJD value by $+17$ d, compared with using SALT2-2014. This caused the recovered Trestmin value (time of earliest observation used in fit, relative to PEAKMJD) to change from -6.6 to $+11$ d – the fitting requires $-20 \leq \text{TRESTMIN} \leq 0$, so SN1298893 was cut from the SALT2-2021 data set, but not the SALT2-2014 data set. In this case, there is a subtle fit instability originating from an initial PEAKMJD estimate that is more than a week off the final SALT2-2014 value. The SALT2-2014 analysis pushes the fit one way, and the SALT2-2021 analysis pushes the fit in the opposite direction, causing a catastrophic fit. This issue is inherent to the light curve fitting process, not the SALT2 surfaces. Following the DES–SN3YR analysis, a more robust pre-fit PEAKMJD estimate has been developed that fixes this catastrophic fit. For this re-analysis, however, we use the original DES–SN3YR fitting algorithms.

4.2 Analysis overview

We perform two analyses – one using SALT2-2014, and the other using SALT2-2021 – to understand the impact of our new SALT2 surface on a cosmology analysis. Each analysis follows Brout et al. (2019b), with the general outline as follows:

(i) We generate detailed simulations (Kessler et al. 2019) for bias corrections.

(ii) We fit light curves from DES–SN3YR data and simulations.

(iii) A BBC fit applies 5D bias corrections, and fits for α, β, and distance moduli (equation 3) averaged in 20 redshift bins.

(iv) We create a (statistical-only) covariance matrix for use in cosmology fitting.

(v) Using binned distances from BBC, we fit a flat wCDM cosmology to measure Ω_m and w. We fit these cosmological parameters using the DES–SN3YR data, combined with Planck Collaboration

XIII (2016) cosmic microwave background (CMB) measurements. We use the fitted cosmological parameters to calculate Δw arising from the change in SALT2 surface, i.e. $\Delta w \equiv w(\text{SALT2-2021}) - w(\text{SALT2-2014})$.

We perform the simulations, light-curve fitting, and bias corrections using SNANA (Kessler et al. 2009a; Kessler et al. 2019), a publicly available supernova analysis software package. The cosmology fitting is performed with CosmoMC (Lewis & Bridle 2002). We run these programs inside the Pippin (Hinton & Brout 2020) pipeline for SN analyses.

4.3 Results

We fit light curves to the DES–SN3YR data and simulations using each surface, and compare the resultant differences in fitted light curve parameters (equation 3) in Figs 6(a)–(c). At this stage of the analysis, bias corrections have not been applied to the fitted light-curve parameters. We find a clear systematic shift in the distribution of supernova colour represented as the βc component. SNe Ia have bluer colours and are brighter when fitted by SALT2-2021, so the change in absolute magnitude (M_{avg}) of -0.024 (Table 3) largely compensates for this change in colour. There is a smaller shift in the distribution of stretch represented as the αx_1 component, most noticeable (but still minor) at higher redshifts. A small systematic shift in the fitted m_B parameter is also shown. The overall fit probability of the light curves tends to improve (i.e. increase) with SALT2-2021, as shown in Fig. 7 – this effect is most significant in the low-redshift subset.

We compute and apply 5D-bias corrections for distance moduli using BBC, with each bias correction simulation generated from the same SALT2 surface used in light-curve fitting. The fitted light-curve parameter distributions for the DES–SN3YR data and the bias correction simulations were compared, and matched well. The recovered nuisance parameters α, β, σ_{int}, and M_{avg}[10] are shown in Table 3 – these change by < 1 per cent.

Fig. 6(d) shows μ before bias corrections are applied. There is a notable shift in μ with the new surface, where the redshift dependence is driven primarily by the changes in the recovered supernova colour (Fig. 6c). There is a further redshift dependence in the bias corrections, shown in Fig. 6(e; discussed further in Appendix B). Overall the change in the bias correction is small compared to the changes in colour and peak absolute magnitude. The total effect of the SALT2-2021 surface on the DES–SN3YR distances is shown by the bias-corrected μ values in Fig. 6(f).

Using CosmoMC results for both surfaces, we find $\Delta w = 0.015$ (Fig. 8).

[9]Available from https://des.ncsa.illinois.edu/releases/sn.

[10]From equation (3). M is calculated and applied for each redshift bin; we report M_{avg} for convenience.
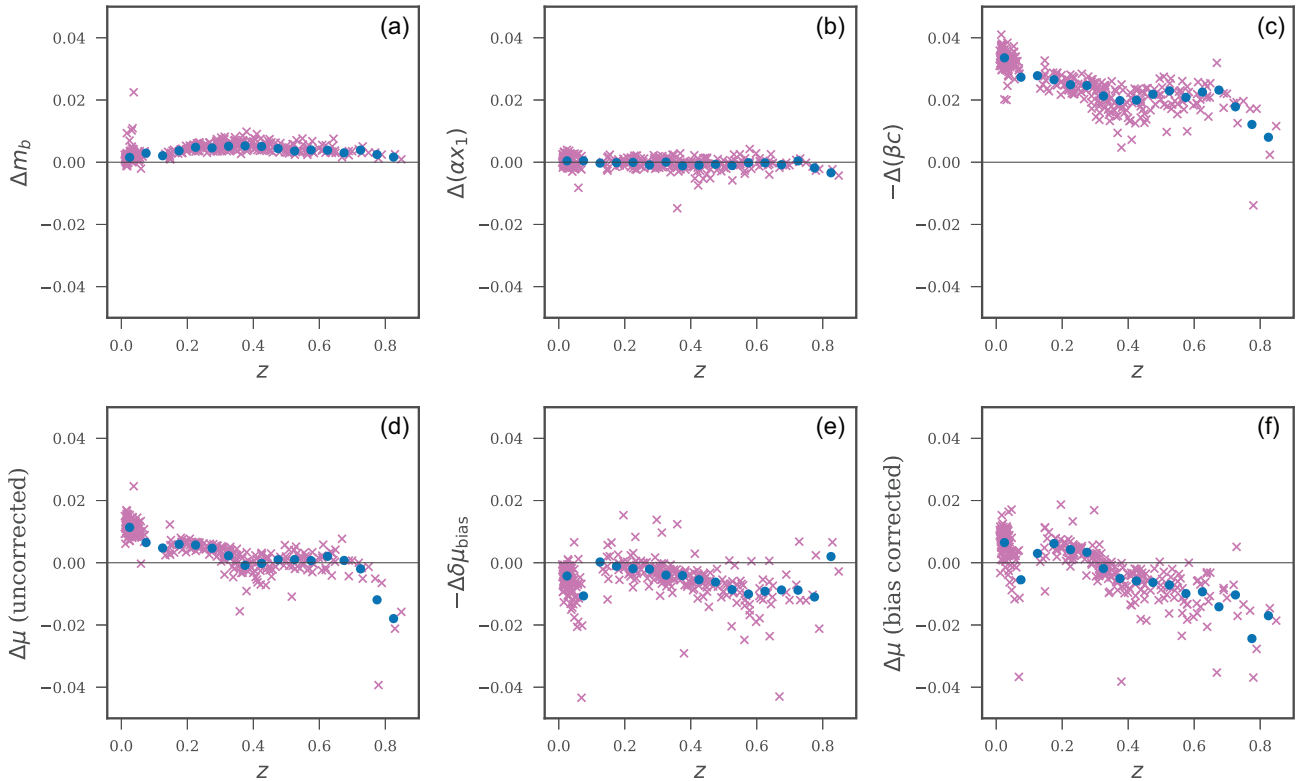
Figure 6. Differences in fitted parameters between the old and new SALT2 surfaces, plotted versus redshift. Differences are given as, e.g. $\Delta\mu = \mu_{2021} - \mu_{2014}$. The top row shows the (uncorrected) supernova parameters as they appear in equation (2): m_B, $\alpha \times$ stretch, and $-\beta \times$ colour. Together with M (where $\Delta M_{avg} = -0.024$, from Table 3), these sum to the (pre-bias corrected) distance modulus. The bottom row shows: pre-bias corrected $\Delta\mu$, the change in bias corrections applied to μ, and $\Delta\mu$ after bias corrections. Note that each term is plotted with its sign according to equation (2), so that the true impact on μ is shown in each panel. Each SN in the fitted sample is plotted as a pink cross, with the binned averages plotted as the blue circles *(nbins = 20)*. One outlier, SN 2007kh, is not displayed.

Table 3. The recovered nuisance parameters for the DES–SN3YR sample using the old and new surfaces.

Surface	α	β	σ_{int}	M_{avg}
SALT2-2014	0.142 ± 0.009	2.99 ± 0.11	0.0979	29.979
SALT2-2021	0.141 ± 0.009	2.97 ± 0.11	0.0985	29.955
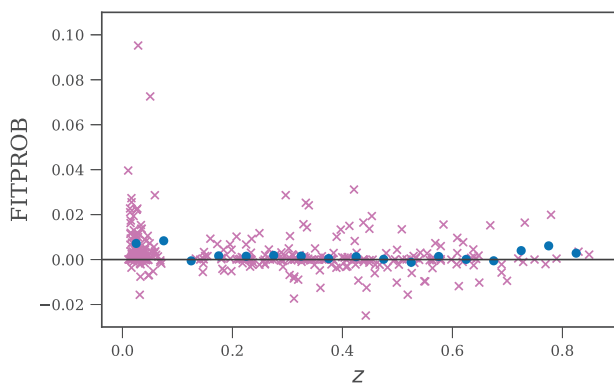
Figure 7. Differences in the FITPROB parameter between the old and new SALT2 surfaces (ΔFITPROB = FITPROB$_{2021}$ − FITPROB$_{2014}$), plotted versus redshift. The FITPROB parameter describes the light-curve fit probability, from 0 to 1. Each SN in the fitted sample is plotted as a pink cross, with the binned averages plotted as blue circles *(nbins = 20)*. One outlier at (0.012, 0.147) is not displayed.
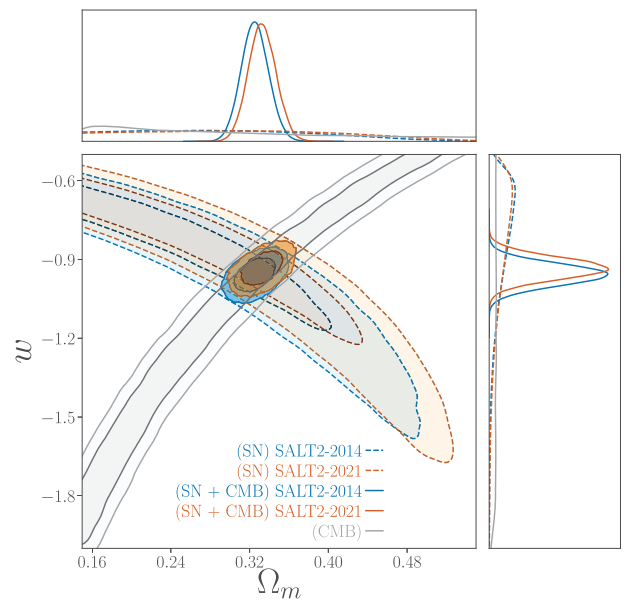
Figure 8. Contour plot showing the difference in cosmology between the old *(blue)* and new *(orange)* SALT2 surfaces. The individual contours for the DES–SN3YR data *(blue and orange dashed)* and the CMB data *(grey solid)* are also shown.
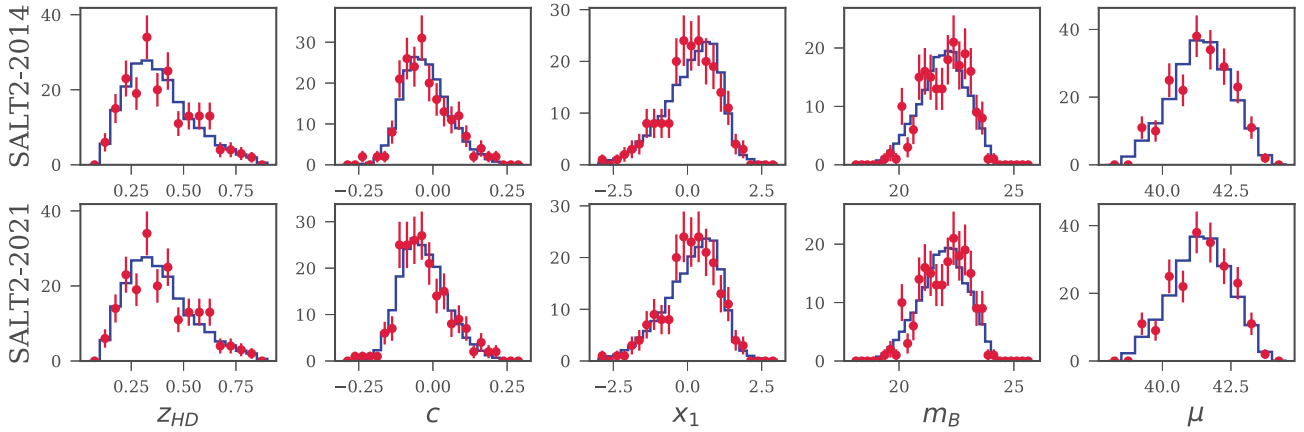
Figure 9. Parameter distributions for DES–SN data *(the red points)* compared with simulated DES SNe Ia *(the blue histograms)*. Simulation histograms are scaled to match the size of the data. The error bars show the Poisson error in binned data.
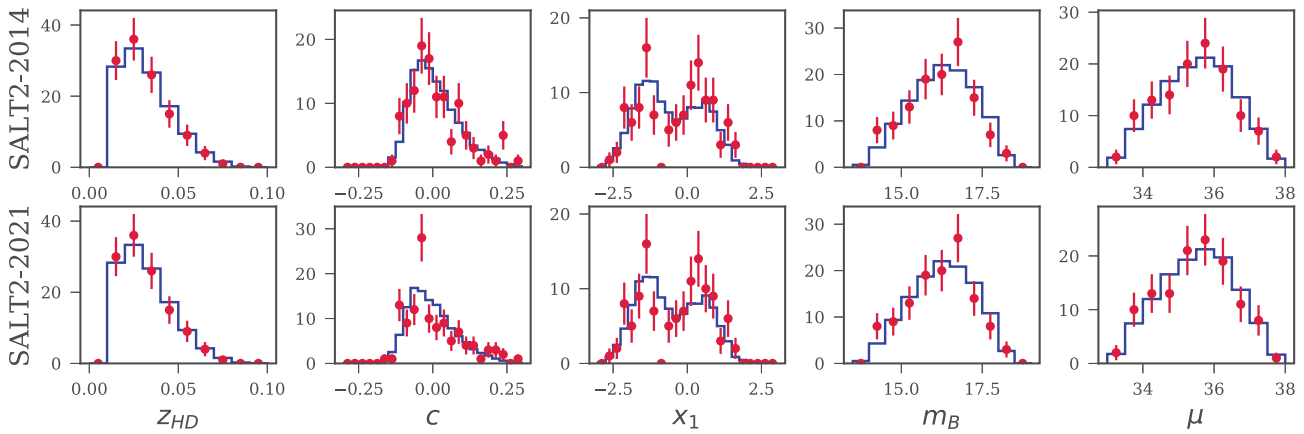
Figure 10. Parameter distributions for low-z data *(the red points)* compared with simulated low-z SNe Ia *(the blue histograms)*. Simulation histograms are scaled to match the size of the data. The error bars show the Poisson error in binned data.

4.4 Simulating uncertainty in w-bias

To estimate the uncertainty in Δw resulting from the change in SALT2 surface, we re-run the analysis on 50 realistic DES–SN3YR-like simulations. Comparisons of various parameter distributions between the data and the simulations are shown in Figs 9 and 10, and agree well. For convenience, we replace CosmoMC with a simpler and faster cosmology fitting program in SNANA (wfit). wfit uses a χ^2 minimization to find w and Ω_m (assuming a wCDM model, i.e. a flat universe with a constant w value and cold dark matter). These parameters are constrained with priors based on the CMB (Hinshaw et al. 2013), and fit with only the simulated SN Ia samples. The w uncertainties produced from wfit are compared to those from CosmoMC (using a *Planck* prior) using DES–SN3YR data, and match well ($\sigma_{\text{wfit}} = 0.046$; $\sigma_{\text{CosmoMC}} = 0.037 - 0.046$). To avoid biases, the computed CMB prior uses the same cosmological parameters as the SN simulations.

From analysing these 50 simulations, we obtain an root mean square (RMS) (for Δw) of 0.004. The Δw values from the simulations are broadly consistent with that recovered from the DES–SN3YR data.

5 DISCUSSION AND CONCLUSIONS

In this paper, we have demonstrated the impact of a revised SALT2 surface on the DES–SN3YR sample. While the overall impact of SALT2-2021 will depend on the specific data sets and analysis

methods used, we see clear impacts from the revised surface for the DES–SN3YR sample.

By reducing the Milky Way extinction by 14 per cent, the SNe in the revised *training* sample have redder intrinsic colours and are fainter, since the corrections are smaller. SALT2-2021 sees a slight change in the average SED, most noticeably at the blue and red ends of the wavelength range (Fig. 4), though these regions are not well constrained in the SALT2 framework with the current training set (Fig. 2). The colour law changes most significantly at the blue end (Fig. 3). The mean $B - V$ colour at B-band maximum is set to be zero for the SNe used in the SALT2 training (Guy et al. 2010). Hence, the colour of a SN will depend on the training sample used to derive a SALT2 surface. This is the origin for the offset seen in Fig. 6(c). On average, the positive residuals indicate that SALT2-2021 lowers the value of c (colour) for SNe Ia in the data sample (i.e. the SNe population becomes bluer).

This effect is largely compensated for by the change in absolute magnitude with the new surface (i.e. the SNe population becomes brighter). The impact of the new surface on the other light curve parameters, x_1 (stretch) and m_B, is small.

These three parameters, along with bias corrections, all contribute to the overall effect on the recovered distance moduli. The change in distance moduli displays a clear redshift dependence, with higher redshift SNe being more affected by the change in SALT2 surface. This is driven mainly by the redshift dependence in the change in supernova colour. A secondary contribution to the redshift dependence

in μ arises from the bias corrections, which is discussed further in Appendix B. The change in the measured distance moduli gives $\Delta w = 0.015 \pm 0.004$ with the SALT2-2021 surface. The impact for the DES–SN3YR sample is comparable to many of the systematic uncertainties quoted in the DES–SN3YR analysis Brout et al. 2019b. The impact of SALT2-2021 on other SNe analyses depends on the sample used and the bias corrections applied.

We have produced a revised surface for the SN Ia model SALT2, which should replace the previous surface for future SNe Ia light-curve fitting. In addition, we provide a suite of linearly perturbed SALT2 surfaces that can be used to estimate the effects of calibration uncertainty in the new model. Further improvements with more complete and high-quality data sets are still possible – in particular, increasing the training sample to include more SNe, particularly in the poorly sampled UV region. Training on the most extensive, high-quality sample available could reduce statistical uncertainties in the SALT2 model. Additionally, removing SNe that are not measured on their natural systems (that is, the system in which they were observed) could further reduce systematic uncertainties in the model. The uncertainties in the SALT2 model have a significant enough effect to be a critical aspect for future SN studies, particularly if they are trying to constrain a time-variable w. In future work, we will examine the systematic and statistical uncertainties of SALT2-2021, and examine how these uncertainties can be reduced by incorporating more modern SNe Ia data sets.

DATA AVAILABILITY

The surface described in this article is publicly available at 10.5281/zenodo.4646495. The data underlying this article are available at https://des.ncsa.illinois.edu/releases/sn.

REFERENCES

Abbott T. M. C. et al., 2018, ApJS, 239, 18
Abbott T. M. C. et al., 2019, ApJ, 872, L30
Bengochea G. R., 2013, preprint (arXiv:1304.6749)
Bernstein J. P. et al., 2012, ApJ, 753, 152
Betoule M. et al., 2014, A&A, 568, A22
Brout D. et al., 2019a, ApJ, 874, 106
Brout D. et al., 2019b, ApJ, 874, 150
Burns C. R. et al., 2011, AJ, 141, 19
Burns C. R. et al., 2014, ApJ, 789, 32
Cardelli J. A., Clayton G. C., Mathis J. S., 1989, ApJ, 345, 245
Chambers K. C. et al., 2016, preprint (arXiv:1612.05560)
Chotard N. et al., 2011, A&A, 529, L4
Conley A. et al., 2008, ApJ, 681, 482
Conley A. et al., 2011, ApJS, 192, 1
Contreras C. et al., 2010, AJ, 139, 519
D'Andrea C. B. et al., 2018, preprint (arXiv:1811.09565)
Dimitriadis G. et al., 2018, ApJ, 870, L1
Fitzpatrick E. L., 1999, PASP, 111, 63
Flaugher B. et al., 2015, AJ, 150, 150
Foley R. J. et al., 2016, MNRAS, 461, 1308–1316
Foley R. J., Hoffmann S. L., Macri L. M., Riess A. G., Brown P. J., Filippenko A. V., Graham M. L., Milne P. A., 2020, MNRAS, 491, 5991
Guy J., Astier P., Nobili S., Regnault N., Pain R., 2005, A&A, 443, 781
Guy J. et al., 2007, A&A, 466, 11
Guy J. et al., 2010, A&A, 523, A7
Hamuy M., Phillips M. M., Suntzeff N. B., Schommer R. A., Maza J., Aviles R., 1996, AJ, 112, 2391
Hamuy M., Trager S. C., Pinto P. A., Phillips M. M., Schommer R. A., Ivanov V., Suntzeff N. B., 2000, AJ, 120, 1479
Hicken M. et al., 2009, ApJ, 700, 331
Hicken M. et al., 2012, ApJS, 200, 12
Hinshaw G. et al., 2013, ApJS, 208, 19
Hinton S. R., 2016, J. Open Source Softw., 1, 00045
Hinton S., Brout D., 2020, J. Open Source Softw., 5, 2122
Holoien T.-S. et al., 2016, MNRAS, 464, 2672–2686
Howell D. A., 2011, Nat. Commun., 2, 350
Jha S. et al., 2006, AJ, 131, 527
Jha S., Riess A. G., Kirshner R. P., 2007, ApJ, 659, 122
Jones D. O. et al., 2018, ApJ, 857, 51
Jones D. O. et al., 2019, ApJ, 881, 19

Kelly P. L., Hicken M., Burke D. L., Mand el K. S., Kirshner R. P., 2010, ApJ, 715, 743

Kessler R., Scolnic D., 2017, ApJ, 836, 56

Kessler R. et al., 2009a, PASP, 121, 1028

Kessler R. et al., 2009b, ApJS, 185, 32

Kessler R. et al., 2013, ApJ, 764, 48

Kessler R. et al., 2015, AJ, 150, 172

Kessler R. et al., 2019, MNRAS, 485, 1171

Khetan N. et al., 2020, Astronomy & Astrophysics, 647, A72

Léget P. F. et al., 2019, Astronomy & Astrophysics, 636, A46

Lewis A., Bridle S., 2002, Phys. Rev. D, 66, 103511

Mandel K. S., Thorp S., Narayan G., Friedman A. S., Avelino A., 2020, preprint (arXiv:2008.07538)

Maoz D., Mannucci F., Nelemans G., 2014, ARA&A, 52, 107

Marriner J. et al., 2011, ApJ, 740, 72

Morganson E. et al., 2018, PASP, 130, 074501

Mosher J. et al., 2014, ApJ, 793, 16

Nobili S., Goobar A., Knop R., Nugent P., 2003, A&A, 404, 901

Phillips M. M., 1993, ApJ, 413, L105

Pierel J. D. R. et al., 2018, PASP, 130, 114504

Planck Collaboration XI, 2014, A&A, 571, A11

Planck Collaboration XIII, 2016, A&A, 594, A13

Pskovskii I. P., 1977, Soviet Astron., 21, 675

Riess A. G., Press W. H., Kirshner R. P., 1996, ApJ, 473, 88

Riess A. G. et al., 1999, AJ, 117, 707

Sako M. et al., 2018, PASP, 130, 064002

Schlafly E. F. et al., 2010, ApJ, 725, 1175

Schlafly E. F., Finkbeiner D. P., 2011, ApJ, 737, 103

Schlafly E. F. et al., 2012, ApJ, 756, 158

Schlegel D. J., Finkbeiner D. P., Davis M., 1998, ApJ, 500, 525

Scolnic D. et al., 2014, ApJ, 795, 45

Scolnic D. et al., 2015, ApJ, 815, 117

Scolnic D. M. et al., 2018, ApJ, 859, 101

Scolnic D. et al., 2020, The Astrophysical Journal, 896, L13

Smith M. et al., 2020, Monthly Notices of the Royal Astronomical Society, 494, 4426

Stritzinger M. D. et al., 2011, AJ, 142, 156

Sullivan M. et al., 2010, MNRAS, 406, 782

Sullivan M. et al., 2011, ApJ, 737, 102

Suzuki N. et al., 2012, ApJ, 746, 85

The Dark Energy Survey Collaboration, 2005, preprint (astro-ph/0510346)

Tripp R., 1998, A&A, 331, 815

Wang X., Wang L., Pain R., Zhou X., Li Z., 2006, ApJ, 645, 488

APPENDIX A: PROCESS VERIFICATION

As a check on our training process, we reproduce the most recent surface, SALT2-2014(JLA), using `snpca`. This is shown in Fig. A1, where our reproduced copy of the surface is denoted SALT2-2014(T21).
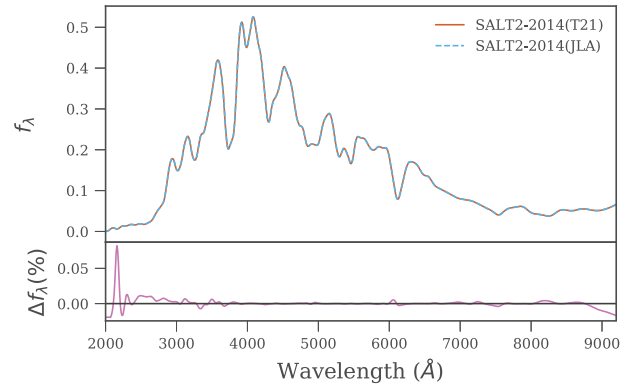

Figure A1. The trained spectral energy distribution of a SN Ia ($c = 0$, $x_1 = 0$) for the SALT2-2014(JLA) surface was reproduced with the accuracy shown above (the two lines are directly overlaid). Our ability to reproduce this surface gives us confidence in the training process.

As a further check, we refit the SN sample in the DES–SN3YR data release[11] (Brout et al. 2019a) using the same SALT2-2014(JLA) version that they used.[12] Differences in the light-curve parameters (and resulting SN distances) between our results and the published results are at the millimag level and are shown in Fig. A2. We have not tracked down the reasons for the differences, but they are small enough to have a negligible impact on the derived distances – note the scale on the axes are an order of magnitude smaller than those from the change in surface in Fig. 6. We therefore have confidence that the training and fitting methods used for the SALT2-2021 surface are consistent with the methods used in the JLA, and any differences from SALT2-2021 are from the revised input data and not from our implementation of the process.

---

[11] Available from https://des.ncsa.illinois.edu/releases/sn.
[12] Available from http://supernovae.in2p3.fr/salt/.
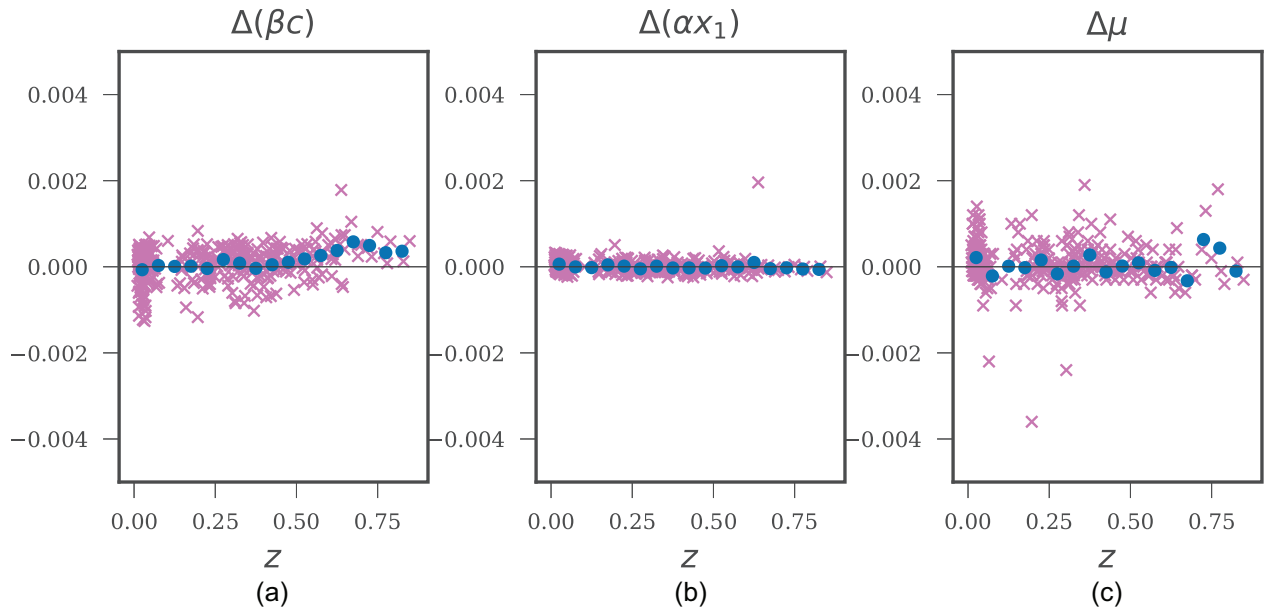
Figure A2. Differences in fitted parameters between the published JLA surface and the JLA surface we trained, plotted versus redshift. Differences are given as, e.g. $\Delta\mu = \mu_{2014(T21)} - \mu_{2014(JLA)}$. Parameters are *(from left to right)*: $\beta \times$ colour, $\alpha \times$ stretch, and μ after bias corrections. Each SN in the fitted sample is plotted as a pink cross, with the binned averages plotted as the blue circles *(nbins=20)*. One $\Delta\mu$ outlier is not shown.

APPENDIX B: ANALYSING BIAS CORRECTIONS

The difference in the recovered (bias-corrected) distance moduli for SALT2-2021 versus SALT2-2014 displays a noticeable redshift dependence, where higher redshift SNe Ia are more affected by the change in surface (Fig. 6f). Some of this redshift dependence comes from the bias corrections applied ($\Delta\delta\mu_{bias}$, Fig. 6e). Here, we briefly examine the reasons for this effect.

Fig. B1 shows the difference in the bias corrections applied for parameters fitted using SALT2-2021 versus SALT2-2014. The *mB* parameter bias correction displays the strongest redshift-dependent trend, and looks to be the main contributor to the effect that we see in Fig. 6(e). Interestingly, there is no obvious redshift-dependent trend in the c bias corrections, though the fitted colour parameters from the DES–SN3YR data show a clear redshift dependence (Fig. 6c). We also note that the redshift-dependent shift in bias corrections persists when performing 1D (rather than 5D) bias corrections on the DES–SN3YR sample.
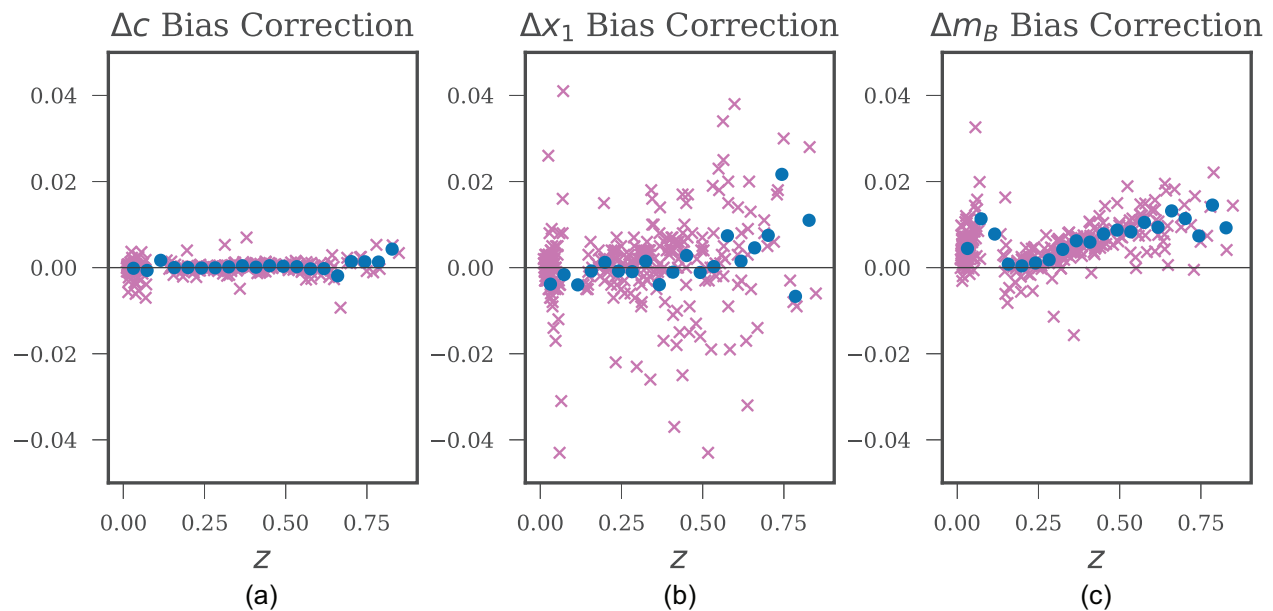
Figure B1. Differences in bias corrections of fitted parameters between the old and new SALT2 surfaces, plotted versus redshift. Differences are given as e.g. $\Delta c = c_{2021} - c_{2014}$. Parameters are *(from left to right)*: colour bias corrections, stretch bias corrections, and m_B bias corrections. Each SN in the fitted sample is plotted as a pink cross, with the binned averages plotted as blue circles *(nbins = 20)*.

We investigate the origins of this redshift-dependent change in bias corrections (caused by the change in SALT2 surface from SALT2-2014 to SALT2-2021) by looking at the bias corrections in the DES–SN3YR data from other SALT2 surfaces. We create 'hybrid' surfaces that combine components (C_L, M_0, M_1) from SALT2-2014 and SALT2-2021, to see if a particular component is responsible for the effect. While the colour law appears to have the strongest effect on the bias corrections, it does not fully explain the shift in bias corrections, which is only seen when using all three SALT2-2021 components in a surface. We also examine the bias corrections when fitting over a restricted wavelength range (4000–7000Å), and rule out fitting data in the UV range as the cause of the redshift-dependent $\Delta\delta\mu_{\rm bias}$. Either the three SALT2-2021 components have some extra effect when applied in combination, or there is some other, unknown factor that is affecting the bias corrections.

This paper has been typeset from a TeX/LaTeX file prepared by the author.